This article has been accepted for publication in a future proceedings of this conference, but has not been fully edited. Content may change prior to final publication. Citation information: DOI: 10.1109/ICASSP49660.2025.10888047, ICASSP 2025 - 2025 IEEE International Conference on Acoustics, Speech and Signal Processing (ICASSP)

Threshold Sensitivity in Two-Channel Modulo ADCs: Analysis and Robust Reconstruction

Wenyi Yan† Lu Gan† Yimin D. Zhang‡
†Dept. of Electrical and Electronic Engineering, Brunel University, London, UK
‡Dept. of Electrical and Computer Engineering, Temple University, Philadelphia, PA, USA

***Abstract*—This paper presents a comprehensive analysis of two-channel modulo analog-to-digital converters (ADCs) systems, focusing on the sensitivity of ADC thresholds. By exploiting analytic number theory, we first investigate the relationship among ADC threshold precision, maximum signal dynamic range, and error tolerance. Our analysis reveals that even slight deviations in ADC thresholds can substantially impact the maximum reconstructed signal dynamic range and error tolerance. To address these sensitivity issues, we propose a novel approach that strategically sacrifices signal dynamic range to stabilise error tolerance in the presence of slight ADC threshold variations. We also introduce a low-complexity reconstruction algorithm that exploits this trade-off, thereby enhancing system robustness. Simulation results validate the theoretical framework and confirm the efficiency of our proposed algorithm.**

***Index Terms*—Analog-to-digital converters (ADCs), modulo samplers, Chinese remainder theorem (CRT), analytic number theory.**

I. Introduction

Conventional analog-to-digital converters (ADCs) saturate when the input signal exceeds the ADC's threshold $\frac{\Delta}{2}$, limiting the output to the range $\left[-\frac{\Delta}{2}, +\frac{\Delta}{2}\right]$, where $\Delta > 0$ is the ADC's peak-to-peak range. Modulo ADCs address this limitation by introducing a folding operation [1]–[11]. For an input $x \in \mathbb{R}$, the modulo (or folding) operation is defined as [12]–[14]:

$$\langle x \rangle_{\Delta} = \Delta \left(\left[\!\!\left[\frac{x}{\Delta} + \frac{1}{2} \right]\!\!\right] - \frac{1}{2} \right), \quad [\![x]\!] \stackrel{\text{def}}{=} x - \lfloor x \rfloor, \tag{1}$$

where $\lfloor \cdot \rfloor$ denotes the floor function. However, in a single-channel modulo-ADC system, the requirement for high sampling rates results in increased data volume, storage demands, and computational costs [1].

In response to these challenges, multi-channel modulo-ADC systems have been proposed in [15]–[17]. Such systems utilise an L-channel framework with progressively increasing ADC ranges $\Delta_1 < \Delta_2 < \cdots < \Delta_L \leq \Delta_{\max}$ defined by:

$$\Delta_l = \epsilon \tau_l, \quad 1 \leq l \leq L, \tag{2}$$

where $L \geq 2$, $\Delta_{\max}$ is the maximum ADC peak-to-peak range, ϵ is a positive floating-point number, and $\tau_1, \cdots, \tau_L$ are pairwise co-prime integers. Each channel is sampled at the Nyquist rate f_{NYQ}, resulting in a total sampling rate of $f_T = L f_{NYQ}$. In the noiseless case, perfect reconstruction is feasible even with $L = 2$ [15]. Hereafter, we focus on a two-channel modulo ADC sampling system due to its low implementation cost.

Given a band-limited input signal $g(t)$, the k-th sample (where $k \in \mathbb{Z}$) is defined as $g_k = g(k/f_{NYQ})$. The k-th modulo sample of the l-th channel, denoted as $\tilde{r}_{k,l}$, is

$$\tilde{r}_{k,l} = \langle g_k \rangle_{\Delta_l} + e_{k,l}, \tag{3}$$

for $l = 1, 2$, where $e_{k,l}$ represents the noise introduced during the sampling process. The recovery algorithm for the multi-channel modulo ADC system, based on the robust Chinese remainder theorem (RCRT) [18]–[20], ensures fast and reliable signal reconstruction. Stable reconstruction is guaranteed if the maximum remainder error $\|\boldsymbol{e}\|_{\infty} = \max_{k,l} |e_{k,l}|$ from the modulo samplers stays within the error bound δ, defined as

$$\|\boldsymbol{e}\|_{\infty} < \delta = \epsilon/4. \tag{4}$$

The dynamic range of signals that can be accurately reconstructed using the RCRT algorithm spans from $[-P, P]$, where the peak recoverable signal magnitude P is determined by

$$P = \frac{\epsilon \tau_1 \tau_2}{2}. \tag{5}$$

In [21], [22], it was demonstrated that, with a ratio Δ_2/Δ_1 being an *irrational number*, the signal dynamic range can be infinite, theoretically enabling *unlimited sampling*. The application of two-channel modulo ADCs for sampling signals with a finite rate of innovation has also been explored [21]–[23]. Furthermore, recent research has investigated the sub-Nyquist sampling of complex exponentials using two-channel modulo ADCs constructed from Gaussian integers [24].

Despite the aforementioned advancements, the implications of ADC threshold deviations have not been addressed in existing studies. For instance, while a threshold may be intended at $1.4V$, various factors such as ADC resolution, reference voltage drift, temperature-induced errors, and noise interference could inadvertently adjust it to $1.41V$ [25]–[29]. Such deviations can critically influence the signal dynamic range and error tolerance of the reconstruction algorithms, yet this crucial issue remains unexplored.

Addressing the aforementioned issues, this paper conducts a comprehensive investigation into ADC threshold deviations, incorporating both theoretical analysis and the development of a robust reconstruction algorithm. Key contributions include:

- An examination of how the precision of ADC thresholds affects the system's maximum recoverable magnitude and error tolerance.

This article has been accepted for publication in a future proceedings of this conference, but has not been fully edited. Content may change prior to final publication. Citation information: DOI: 10.1109/ICASSP49660.2025.10888047, ICASSP 2025 - 2025 IEEE International Conference on Acoustics, Speech and Signal Processing (ICASSP)

- The development of the threshold sensitivity stabilisation algorithm (TSSA), which effectively manages threshold deviations by strategically reducing the signal dynamic range to enhance error tolerance.

The paper is organized as follows: Section II explores the effect of ADC threshold precision on system performance. Section III introduces a robust reconstruction algorithm to stabilise the performance. Section IV provides simulation results validating the proposed algorithm. Section V concludes with a summary and future work.

Notations: The greatest common divisor and least common multiple of integers a and b are denoted by $\gcd(a,b)$ and $\text{lcm}(a,b) = |a \cdot b|/\gcd(a,b)$, respectively. The probability of event A is given by $\mathbb{P}\{A\}$. For an irrational number η, $\beta_m(\eta)$ denotes the operation of truncating η to m decimal places. The asymptotic upper bound of a function is indicated by $\mathcal{O}(\cdot)$. P represents the maximum signal magnitude under RCRT, with δ as the corresponding error bound. $\bar{P}$ and $\bar{\delta}$ denote the signal magnitude and error bound under the proposed TSSA, respectively. The floor and rounding functions are denoted by $\lfloor\cdot\rfloor$ and $\lceil\cdot\rfloor$, while $\text{sgn}(\cdot)$ represents the sign function.

II. Theoretical Bounds: ADC Threshold Precision vs. System Performance

This section uses analytic number theory to study how ADC threshold precision affects the peak signal magnitude and error tolerance in two-channel modulo ADCs.

To this end, let us consider a *deterministic* maximum ADC range, $\Delta_{\max}$, written in scientific notation as $\Delta_{\max} = \Gamma \times 10^{\alpha}$, where $1 \le \Gamma < 10$ achieves precision to the m-th decimal place, i.e., $\Gamma = \sum_{i=0}^{m} \Gamma_i \times 10^{-i}$, with Γ_i representing the i-th decimal digit and α an integer exponent. Alternatively, it may be represented by

$$\Delta_{\max} = \Gamma_{\max} \times 10^{\alpha - m}, \tag{6}$$

where $\Gamma_{\max} = 10^m \times \Gamma$ is a positive integer. For instance, if $\Delta_{\max} = 12$ and $m = 4$, the initial scientific notation is $\Delta_{\max} = 1.2000 \times 10$, with $\Gamma = 1.2000$ and $\alpha = 1$. We then revise this to $\Delta_{\max} = 12000 \times 10^{-3}$ where $\Gamma_{\max} = 12000$. Subsequently, the actual ADC ranges Δ_1 and Δ_2 are modeled as random variables described by

$$\Delta_l = A_l \times 10^{\alpha - m}, \quad l = 1, 2, \tag{7}$$

where A_l are random positive integers selected uniformly and independently from the set $\{1, 2, \cdots, \Gamma_{\max}\}$. Theorem 1 below analyzes the relationship between error bound δ, peak magnitude P, and the number of decimal places m.

Theorem 1. Consider a two-channel modulo ADC sampling system with the maximum ADC range as defined in (6). Let the actual ADC ranges Δ_l, $l = 1, 2$, be given as in (7). Then:

(a) The error bound δ satisfies:

$$\mathbb{P}\left\{\frac{10^{\alpha-m}}{4} \le \delta \le 10^{\alpha-m}\right\} > 86.2\% + \mathcal{O}\left(\frac{\log(\Gamma_{\max})}{\Gamma_{\max}}\right).$$

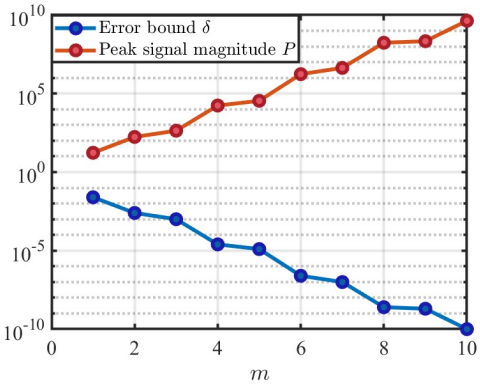

Fig. 1. Error tolerance (δ) and peak signal magnitude (P) and for $\Delta_2 = 2$ and $\Delta_1 = \beta_m(\sqrt{3})$, with number of decimal places m varying from 1 to 10.

(b) The peak signal magnitude P satisfies

$$\mathbb{P}\left\{\frac{\Gamma_{\max}^2 \times 10^{\alpha-m}}{4} < P < \Gamma_{\max}^2 \times 10^{\alpha-m}\right\} > 73\% + \mathcal{O}\left(\frac{\log(\Gamma_{\max})}{\Gamma_{\max}}\right).$$

Proof. From Eqs. (2), (4) and (7), δ is given by

$$\delta = \frac{10^{\alpha-m} \times \gcd(A_1, A_2)}{4}. \tag{8}$$

For two random integers A_1 and A_2 uniformly distributed in $\{1, 2, \cdots, \Gamma_{\max}\}$, the probability that $\gcd(A_1, A_2) = k$ can be expressed as [30], [31]

$$\mathbb{P}\{\gcd(A_1, A_2) = k\} = \frac{6}{\pi^2}\frac{1}{k^2} + \mathcal{O}\left(\frac{\log(\Gamma_{\max})}{\Gamma_{\max}}\right). \tag{9}$$

It can be easily calculated that $\sum_{k=1}^{4} \frac{6}{\pi^2}\frac{1}{k^2} = 86.2\%$, thus Part (a) of the Theorem holds.

For the peak signal magnitude P, Eq. (5) implies

$$P = \frac{10^{\alpha-m} \times \text{lcm}(A_1, A_2)}{2}. \tag{10}$$

As $A_1 < A_2 \le \Gamma_{\max}$, it is clear that $\text{lcm}(A_1, A_2) \le \Gamma_{\max}^2$. According to [32], the probability of $\text{lcm}(A_1, A_2) > t\Gamma_{\max}^2$ is expressed as

$$\begin{aligned}&\mathbb{P}\{\text{lcm}(A_1, A_2) > t\Gamma_{\max}^2\}\\ =&\frac{6}{\pi^2}\sum_{j=1}^{\lfloor 1/t \rfloor}\frac{1 - jt(1 - \log(jt))}{j^2} + \mathcal{O}\left(\frac{\log(\Gamma_{\max})}{\Gamma_{\max}}\right),\end{aligned} \tag{11}$$

where t is a scaling factor. Substituting $t = 1/4$ into (11) completes the proof. ■

When $\Gamma_{\max} \gg 1$, the correction term $\mathcal{O}(\log(\Gamma_{\max})/\Gamma_{\max})$ is usually very small and can be ignored. Part (a) of Theorem 1 indicates that, with high probability, the error bound δ is on the order of $10^{\alpha-m}$. This suggests that δ diminishes ***exponentially*** with m. Similarly, given that $\Gamma_{\max}$ is approximately on the order of 10^{2m}, the peak signal magnitude P is fundamentally on the order of $10^{m+\alpha}$, indicating its ***exponential*** growth with m. Example 1 below further explains this phenomenon.

This article has been accepted for publication in a future proceedings of this conference, but has not been fully edited. Content may change prior to final publication. Citation information: DOI: 10.1109/ICASSP49660.2025.10888047, ICASSP 2025 - 2025 IEEE International Conference on Acoustics, Speech and Signal Processing (ICASSP)

Example 1. Consider a modulo ADC where $\Delta_2 = 2$ and $\Delta_1 = \beta_m(\sqrt{3})$, with $\beta_m(\sqrt{3})$ representing the value of $\sqrt{3}$ retained to m decimal places. At $m = 1$, as $\Delta_1 = \beta_1(\sqrt{3}) = 1.7 = 17 \times 0.1$ and $\Delta_2 = 20 \times 0.1$, indicating $\tau_1 = 17$, $\tau_2 = 20$, and $\epsilon = 0.1$. From Eqs. (4) and (5), we can derive that $\delta = 0.1/4 = 2.5 \times 10^{-2}$ and $P = 20 \times 17 \times 0.1/2 = 17$. Increasing to $m = 2$, Δ_1 adjusts to 1.73, using a similar calculation producing $\delta = 2.5 \times 10^{-3}$ and $P = 173$. Figure 1 demonstrates the variation of δ and P as m increases from 1 to 10, confirming that both metrics exhibit trends consistent with Theorem 1. Notably, even marginal adjustments in ADC dynamic range can significantly influence both the peak signal magnitude and the error tolerance.

III. Robust Reconstruction Algorithm for Stabilizing Error Tolerance

This section presents a robust reconstruction algorithm that mitigates ADC threshold sensitivity by sacrificing signal dynamic range, similar to the concepts described in [33], [34]. Here, we assume that the actual values of Δ_1 and Δ_2 can be obtained through ADC calibration. In the noiseless case, the signal sample g_k can be expressed as

$$g_k = n_{k,l}\Delta_l + \langle g_k \rangle_{\Delta_l}, \quad l = 1, 2,$$

where $n_{k,l}$ are referred to as folding integers. *Robust reconstruction* refers to the accurate estimation of these folding integers from noisy modulo samples $\tilde{r}_{k,l}$ as defined in (3).

To explain the idea, we consider an example with thresholds $\Delta_1 = 1.7$ and $\Delta_2 = 2$. The corresponding peak signal magnitude is $P = 17$ and the error bound is $\delta = 0.025$. Figure 2 illustrates the remainders $r_1 = \langle x \rangle_{1.7}$ and $r_2 = \langle x \rangle_2$ for $-17 \le x \le 17$ on a 2D graph. The intersection r_1-r_2 on the horizontal axis identifies distinct pairs of folding integers $n_1 = (x - r_1)/1.7$ and $n_2 = (x - r_2)/2$ [34]. The full dynamic range is marked by a combination of blue dashed lines and red solid lines covering range $[-17, 17]$. When an error occurs, as shown by the "Error Point" in Figure 2, it deviates from these diagonal lines. A robust reconstruction algorithm is required to accurately map this error point to the appropriate line. By constraining the signal dynamic range to $[-5, 5]$, as indicated by the solid red diagonal lines, the separation between the lines increases to $d_2 = 0.3$ from $d_1 = 4\delta = 0.1$, thereby enhancing error tolerance.

Theorem 2. Consider a two-channel modulo ADC system where the thresholds satisfy $\Delta_1 < \Delta_2 < 2\Delta_1$. Then, the following results hold:

(a) For signal amplitudes within $[-\bar{P}, \bar{P}]$, where

$$\bar{P} = \max\left\{\Delta_2\left(\left\lfloor\frac{\Delta_2}{2\sigma}\right\rfloor - 0.5\right), \Delta_1\left(\left\lfloor\frac{\Delta_1}{2\sigma}\right\rfloor + 0.5\right)\right\}$$

with $\sigma = \Delta_2 - \Delta_1$, the corresponding error bound is $\bar{\delta} = \sigma/4$. This bound is achievable through the application of the TSSA detailed in Algorithm 1.

(b) If $\Delta_2/2 < \Delta_1 < 2\Delta_2/3$, then $\bar{P} = \Delta_2/2$.

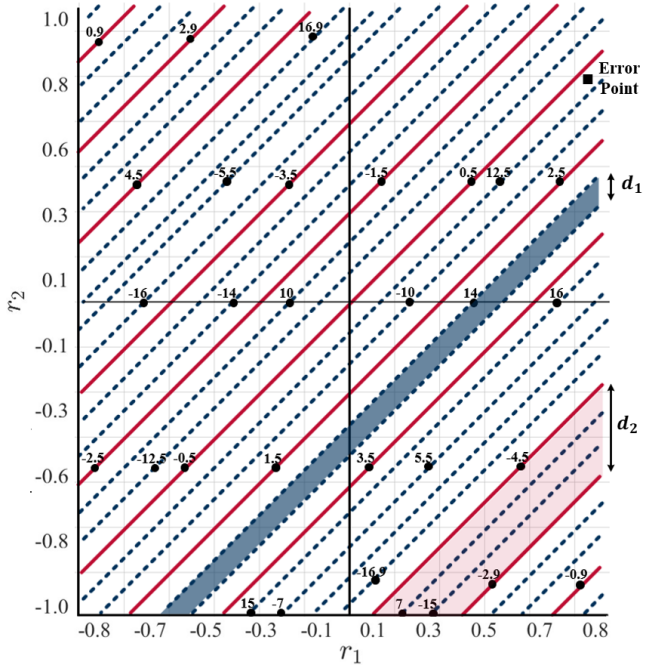

Fig. 2. Remainders are represented with $r_1 = \langle x \rangle_{1.7}$ and $r_2 = \langle x \rangle_2$, where blue dashed and red solid diagonal lines collectively span the entire range of $x \in [-17, 17]$. The solid red diagonal lines exclusively cover the narrower range of $x \in [-5, 5]$.

(c) For thresholds defined by $\Delta_1 = q\epsilon$ and $\Delta_2 = (q+1)\epsilon$ with $q \ge 2$ being a positive integer, we find $\bar{P} = P = q(q+1)\epsilon/2$ and $\bar{\delta} = \delta = \epsilon/4$.

Proof. Due to lack of space, we present only an outline of the main proof steps. In **Part (a)**, the derivations for $\bar{P}$ and $\bar{\delta}$ employ methods akin to those in Theorem 1 from [33] and Proposition 3 from [34]. Our proposed TSSA is a refinement of Algorithm 1 in [34]. The main distinctions are twofold: Firstly, prior studies generate a modulo remainder within $[0, \Delta)$, whereas Eq. (1) yields a range of $[-\Delta/2, \Delta/2)$. Secondly, we introduce the condition $\Delta_2 < 2\Delta_1$ to effectively utilise the ADC's dynamic range, thereby enhancing the recoverable signal range. For **Part (b)**, verification is straightforward by observing that $\lfloor \Delta_1/(2\sigma) \rfloor = 0$ when $\Delta_2/2 < \Delta_1 < 2\Delta_2/3$. **Part (c)** is substantiated by separate analyses for cases when $q = 2q_0$ and $q = 2q_0 + 1$, where q_0 is a positive integer. ■

Part (a) of Theorem 2 demonstrates that $\bar{P}$ and $\bar{\delta}$ are determined by Δ_1 and Δ_2, and their difference σ. This arrangement assures stability in signal reconstruction despite minor threshold fluctuations, as we will show in Section IV. **Part (b)** implies that, when $\Delta_2/2 < \Delta_1 < 2\Delta_2/3$, the output from the second ADC channel faithfully reproduces the input signal ($\tilde{r}_{k,2} = \tilde{g}_k$), rendering the output from the first channel ($\tilde{r}_{k,1}$) unnecessary. This setup implies that the TSSA operates efficiently only if $\Delta_1 > 2\Delta_2/3$; therefore, Δ_1 should not be too low to maintain system efficacy. **Part (c)** discusses a specific configuration of Δ_l for $l = 1, 2$, where the TSSA achieves a dynamic range equivalent to that of the RCRT

This article has been accepted for publication in a future proceedings of this conference, but has not been fully edited. Content may change prior to final publication. Citation information: DOI: 10.1109/ICASSP49660.2025.10888047, ICASSP 2025 - 2025 IEEE International Conference on Acoustics, Speech and Signal Processing (ICASSP)

Algorithm 1 Threshold sensitivity stabilisation algorithm

Input: $\tilde{r}_{k,1}, \tilde{r}_{k,2}, \Delta_1, \Delta_2$

Output: Recovered estimate $\tilde{g}_k$

$q_k \leftarrow \tilde{r}_{k,1} - \tilde{r}_{k,2}$ and $\sigma \leftarrow \Delta_2 - \Delta_1$

$\tilde{n}_k \leftarrow \left\lfloor \frac{\Delta_1}{2\sigma} \right\rfloor$

▷ Calculate the folding integer $\tilde{n}_{k,2}$

if $|q_k| \leq \sigma(\tilde{n}_k + 0.5)$ **then**

$$\tilde{n}_{k,2} \leftarrow \left\lceil \frac{q_k}{\sigma} \right\rfloor$$

else

$$\tilde{n}_{k,2} \leftarrow -\text{sgn}(q_k) \cdot \left\lceil \frac{\Delta_1 - |q_k|}{\sigma} \right\rfloor$$

end

▷ Calculate the folding integer $\tilde{n}_{k,1}$

$$\tilde{n}_{k,1} \leftarrow \left\lceil \frac{\tilde{n}_{k,2}\Delta_2 + \tilde{r}_{k,2} - \tilde{r}_{k,1}}{\Delta_1} \right\rfloor$$

$\tilde{g}_k \leftarrow \frac{1}{2}\sum_{l=1}^{2} (\tilde{n}_{k,l}\Delta_l + \tilde{r}_{k,l})$

algorithm. As noted in [17], this arrangement of Δ_l yields an optimal error bound δ for given $\Delta_{\max}$ and P.

IV. Simulation Results

This section presents simulation results to validate Theorem 2 and the proposed TSSA. The performance is compared to the RCRT algorithm [18].

We first fix $\Delta_2 = 8 \times 0.2 = 0.16$ and vary Δ_1 around 0.14, as shown in Table I. It can be observed that, when $\Delta_1 = 7 \times 0.2 = 0.14$, TSSA produces the same signal dynamic range and error bound as RCRT, consistent with Part (c) of Theorem 2. When Δ_1 slightly increases from 0.14 to 0.141, the RCRT algorithm exhibits a significant expansion in dynamic range, from $[-0.56, 0.56]$ to $[-11.28, 11.28]$. However, this increase in dynamic range is accompanied by a notable reduction in error tolerance, which decreases from 5×10^{-3} to 2.5×10^{-4}. Similar trends are observed for other settings of Δ_1 being 0.147, 0.133, and 0.1395, respectively. In contrast, the proposed TSSA algorithm shows much greater stability under similar conditions, with $\bar{P}$ and $\bar{\delta}$ remaining within the same order of magnitude.

Figure 3 presents numerical simulations comparing the performance of the proposed TSSA and RCRT under quantisation noise. We evaluated three sets of modulo ADC peak-to-peak ranges: (i) $\Delta_1 = 0.14$, $\Delta_2 = 0.16$; (ii) $\Delta_1 = 0.141$, $\Delta_2 = 0.16$; and (iii) $\Delta_1 = 0.139$, $\Delta_2 = 0.161$. Each sample was uniformly quantised across a range between 2 and 12 bits. Since both TSSA and RCRT use point-by-point recovery, we conducted simulations by randomly selecting g_k within the interval $[-0.56, 0.56]$. The experiment was repeated 10^4 times to ensure statistical reliability. Performance was evaluated by calculating the mean absolute error (MAE), $E(|\hat{g}_k - g_k|)$, across all trials. It is observed that RCRT produces high MAE values for cases (ii) and (iii). These results illustrate RCRT's sensitivity to threshold variations, requiring more bits to maintain acceptable MAE, while TSSA shows remarkable stability, maintaining error tolerance comparable to optimal conditions, i.e., $\Delta_1 = 0.14$ and $\Delta_2 = 0.16$. These findings underscore TSSA's robustness against threshold deviations. Additionally, unlike the RCRT, our proposed TSSA does not require the computation of modulo inverses, offering a low-cost advantage.

TABLE I
Comparison of signal recoverable range and error tolerance bound with deviations in Δ_1 and fixed $\Delta_2 = 0.16$

Δ_1	Algorithm	Signal Recoverable Range	Error Bound
0.14	RCRT [18]	[-0.56, 0.56]	5×10^{-3}
	TSSA	[-0.56, 0.56]	5×10^{-3}
0.141	RCRT [18]	[-11.28, 11.28]	2.5×10^{-4}
	TSSA	[-0.56, 0.56]	4.8×10^{-3}
0.147	RCRT [18]	[-11.76, 11.76]	2.5×10^{-4}
	TSSA	[-0.88, 0.88]	3.3×10^{-3}
0.133	RCRT [18]	[-10.64, 10.64]	2.5×10^{-4}
	TSSA	[-0.33, 0.33]	6.8×10^{-3}
0.1394	RCRT [18]	$[-55.76, 55.76]$	5×10^{-5}
	TSSA	$[-0.48, 0.48]$	5.2×10^{-3}

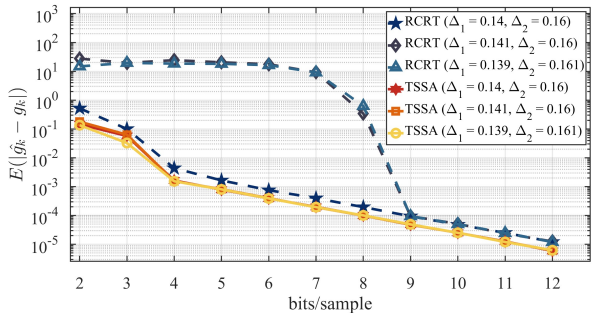

Fig. 3. Mean Absolute Error (MAE) comparison of the proposed TSSA and RCRT [18] under quantisation noise (2 to 12 bits/sample) across three sets of modulo ADC thresholds. Data is based on 10^4 trials with input samples g_k uniformly distributed in $[-0.56, 0.56]$.

V. Conclusion

This paper analyzes the significant impact of minor threshold variations on the performance of two-channel modulo ADC systems. While such variations can greatly increase the dynamic range, they also significantly reduce error tolerance. To address this issue, we propose a low-complexity algorithm that maintains stable error tolerance by adjusting the signal's dynamic range. The algorithm was tested under conditions of quantisation noise, and its robustness was demonstrated through both theoretical analysis and simulations. In the future, we plan to enhance the algorithm's capability to handle a broader dynamic range and evaluate its performance in real hardware implementations.

REFERENCES

[1] Ayush Bhandari, Felix Krahmer, and Ramesh Raskar, "Unlimited sampling of sparse signals," in *Proceedings of 2018 IEEE International Conference on Acoustics, Speech and Signal Processing (ICASSP)*, Calgary, Alberta, Canada, 2018, pp. 4569–4573.

[2] Ayush Bhandari, "Unlimited sampling with sparse outliers: Experiments with impulsive and jump or reset noise," in *Proceedings of 2022 IEEE International Conference on Acoustics, Speech and Signal Processing (ICASSP)*, Singapore, 2022, pp. 5403–5407.

[3] Gal Shtendel, Dorian Florescu, and Ayush Bhandari, "Unlimited sampling of bandpass signals: Computational demodulation via undersampling," *IEEE Transactions on Signal Processing*, vol. 71, pp. 4134–4145, 2023.

[4] Thomas Feuillen, Bhavani Shankar MRR, and Ayush Bhandari, "Unlimited sampling radar: Life below the quantization noise," in *Proceedings of 2023 IEEE International Conference on Acoustics, Speech and Signal Processing (ICASSP)*, Rhodes Island, Greece, 2023, pp. 1–5.

[5] Ruiming Guo and Ayush Bhandari, "ITER-SIS: Robust unlimited sampling via iterative signal sieving," in *Proceedings of 2023 IEEE International Conference on Acoustics, Speech and Signal Processing (ICASSP)*, Rhodes Island, Greece, 2023, pp. 1–5.

[6] Dorian Florescu and Ayush Bhandari, "Time encoding via unlimited sampling: Theory, algorithms and hardware validation," *IEEE Transactions on Signal Processing*, vol. 70, pp. 4912–4924, 2022.

[7] Dorian Florescu and Ayush Bhandari, "Unlimited sampling via generalized thresholding," in *2022 IEEE International Symposium on Information Theory (ISIT)*, Espoo, Finland, 2022, pp. 1606–1611.

[8] Ayush Bhandari, "Back in the US-SR: Unlimited sampling and sparse super-resolution with its hardware validation," *IEEE Signal Processing Letters*, vol. 29, pp. 1047–1051, 2022.

[9] Ziang Liu, Ayush Bhandari, and Bruno Clerckx, "λ–MIMO: Massive MIMO via modulo sampling," *IEEE Transactions on Communications*, vol. 71, no. 11, pp. 6301–6315, 2023.

[10] Matthias Beckmann, Ayush Bhandari, and Meira Iske, "Fourier-domain inversion for the modulo radon transform," *IEEE Transactions on Computational Imaging*, vol. 10, pp. 653–665, 2024.

[11] Dongwon Park, Jehyuk Rhee, and Youngjoong Joo, "A wide dynamic-range CMOS image sensor using self-reset technique," *IEEE Electron Device Letters*, vol. 28, pp. 890–892, 10 2007.

[12] Ayush Bhandari, Felix Krahmer, and Ramesh Raskar, "On unlimited sampling," in *Proceedings of 2017 International Conference on Sampling Theory and Applications (SampTA)*, 2017, pp. 31–35.

[13] Ayush Bhandari, Felix Krahmer, and Ramesh Raskar, "On unlimited sampling and reconstruction," *IEEE Transactions on Signal Processing*, vol. 69, pp. 3827–3839, 2021.

[14] Ayush Bhandari, Felix Krahmer, and Thomas Poskitt, "Unlimited sampling from theory to practice: Fourier-prony recovery and prototype ADC," *IEEE Transactions on Signal Processing*, vol. 70, pp. 1131–1141, 2022.

[15] Lu Gan and Hongqing Liu, "High Dynamic range sensing using multi-channel modulo samplers," in *Proceedings of 2020 IEEE 11th Sensor Array and Multichannel Signal Processing Workshop (SAM)*, 2020, pp. 1–5.

[16] Yicheng Gong, Lu Gan, and Hongqing Liu, "Multi-channel modulo samplers constructed from Gaussian integers," *IEEE Signal Processing Letters*, vol. 28, pp. 1828–1832, 2021.

[17] Wenyi Yan, Lu Gan, Shaoqing Hu, and Hongqing Liu, "Towards optimized multi-channel modulo-ADCs: Moduli selection strategies and bit depth analysis," in *Proceedings of 2024 IEEE International Conference on Acoustics, Speech and Signal Processing (ICASSP)*, Seoul, Korea, 2024, pp. 9496–9500, IEEE.

[18] Wenjie Wang and Xiang-Gen Xia, "A closed-form robust Chinese remainder theorem and its performance analysis," *IEEE Transactions on Signal Processing*, vol. 58, no. 11, pp. 5655–5666, 2010.

[19] Li Xiao and Xiang-Gen Xia, "Error correction in polynomial remainder codes with non-pairwise coprime moduli and robust Chinese remainder theorem for polynomials," *IEEE Transactions on Communications*, vol. 63, no. 3, pp. 605–616, 2015.

[20] Hanshen Xiao, Yufeng Huang, Yu Ye, and Guoqiang Xiao, "Robustness in Chinese remainder theorem for multiple numbers and remainder coding," *IEEE Transactions on Signal Processing*, vol. 66, no. 16, pp. 4347–4361, 2018.

[21] Ruiming Guo and Ayush Bhandari, "Unlimited sampling of FRI signals independent of sampling rate," in *Proceedings of 2023 IEEE International Conference on Acoustics, Speech and Signal Processing (ICASSP)*, Rhodes Island, Greece, June 2023, pp. 1–5.

[22] Yuliang Zhu, Ruiming Guo, Peiyu Zhang, and Ayush Bhandari, "Frequency estimation via sub-Nyquist unlimited sampling," in *Proceedings of 2024 IEEE International Conference on Acoustics, Speech and Signal Processing (ICASSP)*, Souel, Korea, 2024, pp. 9636–9640.

[23] Satish Mulleti and Yonina C. Eldar, "Modulo sampling of FRI signals," *IEEE Access*, vol. 12, pp. 60369–60384, 2024.

[24] Václav Pavlíček, Ruiming Guo, and Ayush Bhandari, "Bits, channels, frequencies and unlimited sensing: Pushing the limits of sub-Nyquist prony," in *Proceedings of the 2024 European Signal Processing Conference (EUSIPCO)*, London, UK, 2024.

[25] Yun-Shiang Shu, Jui-Yuan Tsai, Ping Chen, Tien-Yu Lo, and Pao-Cheng Chiu, "A background calibration technique for fully dynamic flash ADCs," in *Proceedings of 2013 International Symposium on VLSI Design, Automation, and Test (VLSI-DAT)*, Hsinchu, Taiwan, 2013, pp. 1–4.

[26] Baozhen Chen, "A scheme for wide input range precision SAR ADC," in *Proceedings of 2017 IEEE 60th International Midwest Symposium on Circuits and Systems (MWSCAS)*, Boston, MA, 2017, pp. 1029–1032.

[27] Hang Liu, Yuying Li, Haoyuan Shen, Bo Wu, Yu Jin, Duli Yu, and Heming Sun, "An ultra-high linear digitization temperature sensor based on SAR ADC with common-mode temperature drift suppression," *IEEE Transactions on Circuits and Systems II: Express Briefs*, vol. 71, no. 3, pp. 1047–1051, 2024.

[28] Fábio Rabuske, Taimur Rabuske, and Jorge Fernandes, "A 5-bit 300–900-ms/s 0.8–1.2-V supply voltage ADC with background self-calibration," *IEEE Transactions on Circuits and Systems II: Express Briefs*, vol. 64, no. 1, pp. 1–5, 2017.

[29] Guoquan Sun, Yin Zhang, Lenian He, and Xiaolei Zhu, "A threshold control technique for CMOS comparator design," in *Proceedings of 2014 IEEE International Conference on Electron Devices and Solid-State Circuits*, Chengdu, China, 2014, pp. 1–2.

[30] Eckford Cohen, "Arithmetical functions of a greatest common divisor, iii. cesàro's divisor problem," *Proceedings of the Glasgow Mathematical Association*, vol. 5, no. 2, pp. 67–75, 1961.

[31] Persi Diaconis and Paul Erdös, "On the distribution of the greatest common divisor," *Lecture Notes-Monograph Series*, vol. 45, pp. 56–61, 2004.

[32] Sungjin Kim, "On the distribution of the lcm of k-tuples and related problems," *Functiones et Approximatio Commentarii Mathematici*, vol. 68, no. 1, pp. 19 – 39, 2023.

[33] Behrooz Parhami, "Digital arithmetic in nature: Continuous-digit RNS," *The Computer Journal*, vol. 58, no. 5, pp. 1214–1223, May 2015.

[34] Li Xiao, Xiang-Gen Xia, and Haiye Huo, "Towards robustness in residue number systems," *IEEE Transactions on Signal Processing*, vol. 65, no. 6, pp. 1497–1510, 2017.